

## Magnetic-flux dynamics of high- $T_c$ superconductors in weak magnetic fields

E. V. Il'ichev\* and C. S. Jacobsen

*Physics Department, The Technical University of Denmark, DK-2800 Lyngby, Denmark*

(Received 7 April 1993; revised manuscript received 26 October 1993)

Aspects of magnetic-flux dynamics in different types of samples of the high-temperature superconductor  $\text{YBa}_2\text{Cu}_3\text{O}_x$  have been investigated in magnetic fields below 1 Oe and at 77 K. The experiments were carried out in an arrangement including a field coil, a flat sample perpendicular to the field, and a radio frequency-superconducting quantum interference device (RF-SQUID) along a common axis. For epitaxial thin films the Meissner effect was established. For a ceramic sample it was found that field changes of order  $10^{-2}$  Oe affect the flux distribution inside the sample. The observations can explain why RF-SQUID's made from this ceramic operate in the nonhysteretic mode. The central object was an epitaxial film with a large density of defects. In this film the dynamics of the mixed state show features expected in "spin-glass" models.

### I. INTRODUCTION

Due to the intrinsic inhomogeneous nature of high-temperature superconductors the field penetrated mixed state has been described either in terms of effective-medium theories (i.e., as media consisting of grains coupled by the Josephson interaction), or in terms of continuum models which include distributions of inhomogeneities that act as pinning centers for vortices.<sup>1,2</sup> Both types of models can qualitatively account for the high level of flux creep and the relaxation behavior, typically with very slow approach to equilibrium. Therefore many experimental results deal with the nonequilibrium mixed state. The aim of this work is to experimentally study nonequilibrium magnetic-flux dynamics for very small changes in the applied magnetic field.

### II. EXPERIMENT

The schematics of the measuring system is shown in Fig. 1. The coil to the left is the source of applied field. The external diameter is 1 mm, and the coil is made of 30 windings of copper wire, 0.09 mm in diam, yielding a coil center field of 100 Oe/A. A high- $T_c$  radio frequency superconducting quantum interference device (RF-SQUID) is positioned 3 mm from the end of the coil and on the

same axis. The SQUID is manufactured from a  $\text{YBa}_2\text{Cu}_3\text{O}_x$  ceramic disk 2 mm in diam and 2 mm thick. A 0.4-mm-diam hole has been drilled in the center, while in the lateral surface a slit has been cut leaving a bridge with minimum dimensions of 20–30  $\mu\text{m}$ . The SQUID is shown schematically to the right in Fig. 1. Flat samples of typical size  $5 \times 5 \text{ mm}^2$  and varying thickness were inserted between the coil and the SQUID. The RF-SQUID was coupled to a tank circuit biased with a 30 MHz current. The voltage over the circuit was amplified and monitored as a function of the magnet coil current. The coil field profile along the axis was calculated. Furthermore, a calibration was performed by monitoring the SQUID response without any sample. From the period we deduce a current change of  $170 \mu\text{A}/\Phi_0$ , where  $\Phi_0$  is the flux quantum ( $=2.07 \times 10^{-7} \text{ Gcm}^2$ ), consistent with the calculated profile and the cross-sectional area of the SQUID.

All the measurements were carried out in liquid nitrogen ( $T=77 \text{ K}$ ). The experimental space was shielded with a 10-cm-long  $\text{YBa}_2\text{Cu}_3\text{O}_x$  tube of 12 mm internal and 18 mm external diameter. Thus absolute zero for the magnetic field was not established. Only changes in magnetic field were controlled.

The small field coil and demagnetization factors of order unity prevent the field near the edge of the samples to be estimated, but indeed the experiment is designed to have optimum sensitivity for motion of flux lines near the center of the samples.

Three kinds of samples were studied: (1) Epitaxial thin films, obtained by laser deposition on  $\text{SrTiO}_3$  substrates of size  $5 \times 5 \times 0.5 \text{ mm}^3$ . The film thickness is about 200 nm, and the critical current density at 77 K is of order  $10^6 \text{ A/cm}^2$ . (2) A ceramic plate of dimensions  $5 \times 5 \times 1.6 \text{ mm}^3$ . The critical current density at 77 K is about  $70 \text{ A/cm}^2$  (fairly low for a ceramic). (3) A defect-rich epitaxial thin film, which was obtained by a nonoptimized laser deposition process. The film was deposited on a  $5 \times 5 \times 0.5 \text{ mm}^3 \text{ MgO}$  substrate. The film thickness is again  $\sim 200 \text{ nm}$  and the critical current density at 77 K is  $2.5 \times 10^3 \text{ A/cm}^2$ . Figure 2 shows a scanning electron mi-

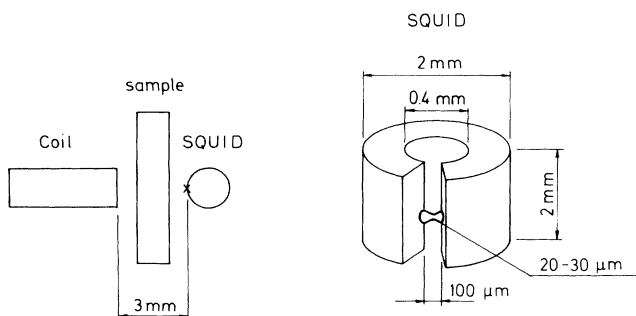


FIG. 1. Schematic drawing of the experiment (left) and the design of the SQUID (right).

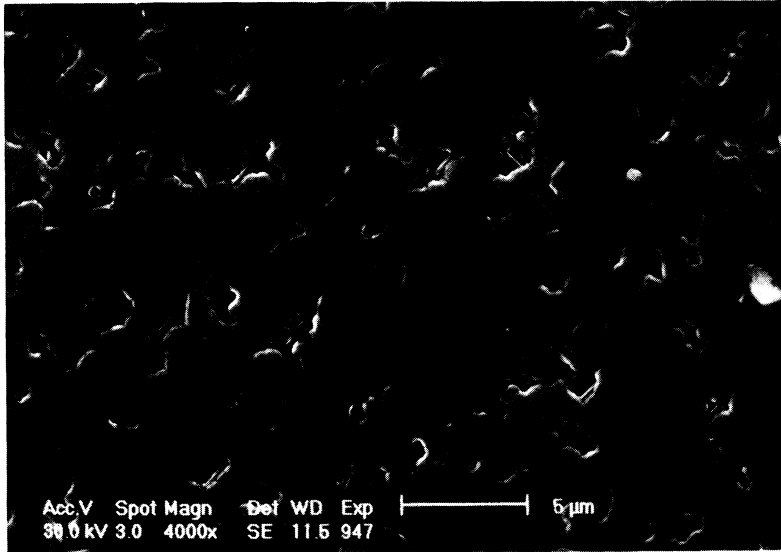


FIG. 2. Scanning electron micrograph of the defect-rich thin film.

crograph of the surface of this film. Note that there are lots of defects (holes) between epitaxial clusters.

### III. RESULTS

The different sample configurations are shown in Fig. 3, while representative experimental results are presented in Fig. 4 as the number of flux quanta detected at the SQUID versus coil current. One flux quantum corresponds to a field change of  $1.6 \times 10^{-4}$  Oe at the SQUID. A number of points has been extracted from the continuous SQUID response curves to make the behavior clear. In all cases, the field was swept up and down repeatedly, with a period of about 10 s. The curves in Fig. 4 were taken with increasing field. Hysteretic effects were ob-

served in some cases and will be commented upon below.

We now describe the results of Fig. 4. Curve 1 is the basic reference described above showing the response in absence of any sample. Curves 2 and 3 are for an epitaxial thin film and for the defect-rich thin film, respectively. The geometrical arrangement is like that shown in Fig. 3(a). The fact that curve 2 is a straight line suggests that the epitaxial film shows nearly perfect shielding. The shielding factor is the ratio between the slopes of curves 1 and 2 and is estimated to be 15. The measured field, when the film is present, may be assumed mainly to originate from field lines circumventing the sample. To verify this a second epitaxial film was checked. It showed a shielding factor of 13, while two joining epitaxial films [Fig. 3(b)] again had a shielding factor of 15. Additionally, it

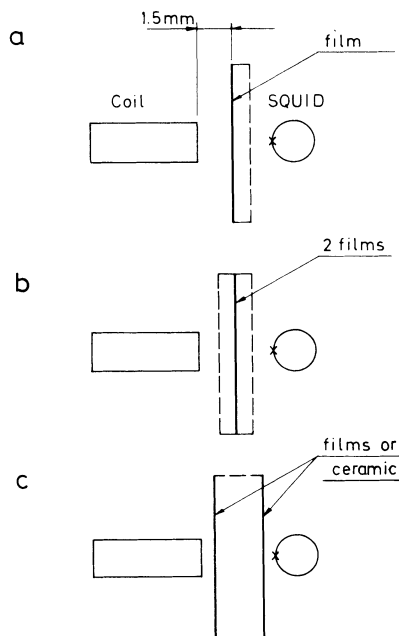


FIG. 3. The sample configurations used in the measurements.

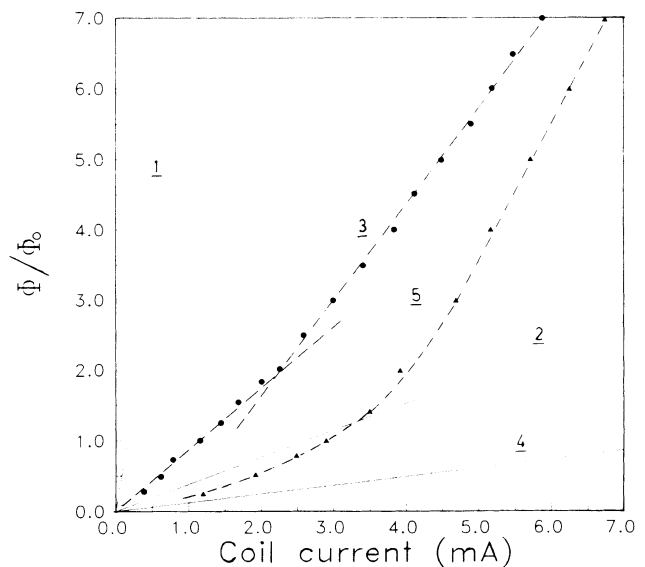


FIG. 4. Flux change detected at SQUID position versus applied coil current. 1: No sample. 2: Epitaxial film. 3: Defect-rich film. 4: Two epitaxial films in positions as to establish a reference for the ceramic sample. 5: Ceramic sample.

was investigated whether hysteretic effects could be observed by (1) moving the thin film as close to the field coil as possible, and (2) by superimposing a static field of 5 Oe (frozen-in field in the surrounding shield). In no instance was hysteresis observed. Finally, the epitaxial films were studied by an optical method, which utilizes the magneto-optical Faraday effect in EuSe films, or employs ferromagnetic garnet films, both in connection with polarized light.<sup>3</sup> The epitaxial films show no sign of field penetration in fields below 5 Oe and full penetration (as judged from this technique) only in fields of order 1 kOe. Thus the use of the films as references is fully justified.

Using the shielding factor defined above we now expect that film samples with defects, which allow penetration in low fields, will have shielding factors between 1 and 15. This is indeed what is observed in curve 3, which also shows a characteristic discontinuous change of slope. This position of the change of slope is hysteretic: On reducing the applied field on the upper part of the curve, the response immediately reverts to the lower slope (higher shielding factor). If on the other hand we stay on the lower part of the curve, the response is reversible. These features are discussed below.

In much the same way we can establish a point of reference for the ceramic sample. The geometry of this sample may be modeled using two epitaxial films with a distance [see Fig. 3(c)]. The response is shown as curve 4 in Fig. 4, thus in this case the factor for perfect shielding is found to be 48. The larger value is obviously due to the sample thickness and to one side being closer to the field coil. Finally, curve 5 shows the response with the ceramic sample in the geometry of Fig. 3(c). Obviously the ceramic can only shield very small field changes efficiently. The curve shows deviations from linear behavior for a very small,  $<2$  mA, increase in coil current. The response for the ceramic sample is distinctly hysteretic when the current sweep direction is changed as the sample tries to maintain its flux configuration. In this sense the ceramic sample behaves as would be expected from the Bean critical state model.<sup>4</sup>

#### IV. DISCUSSION

Let us first discuss the results obtained with the ceramic sample, see Fig. 4, curve 5. The point of deviation from linear behavior corresponds for the present sample position (1 mm from the end of the coil) to an on-axis sample field change of order  $10^{-2}$  Oe. Thus a magnetic-field change of  $\sim 10^{-2}$  Oe is able to change the flux distribution in the central part of the sample.

It is of some interest to discuss this result in the context of operating ceramic RF-SQUID's as the one used in this study (which is manufactured from the same type of ceramic). In this SQUID a change in flux of  $\Phi_0$  corresponds to a field change of  $10^{-4}$  Oe. Since the linear dimension of the bridge in the SQUID is two orders of magnitude smaller than the length of the bulk, the current concentration in the bridge will give a field enhancement at the bridge of order  $10^2$ . This means that the field change corresponding to one flux quantum is  $\sim 10^{-2}$  Oe, just enough to move a vortex through the bridge. This really means that the flux in the SQUID is

changed without vortex jumping: There is a reversible, nondissipative relation between the applied flux and the total flux in the SQUID, as indicated schematically in curve 2 in Fig. 5. If the critical current is somewhat higher (requires  $I_C > \Phi_0/2\pi L$ , where  $L$  is the SQUID inductance<sup>5</sup>), the behavior is hysteretic, as indicated in curve 1 in Fig. 5.

Indeed, the nonhysteretic mode has been observed in several ceramic  $\text{YBa}_2\text{Cu}_3\text{O}_7$  RF-SQUID's, both at helium temperatures,<sup>6,7</sup> and at nitrogen temperatures.<sup>8</sup> The RF-SQUID used in this study is also nonhysteretic. Its signal properties have been investigated in detail.<sup>9</sup>

Now let us turn to the defect-rich thin film, curve 3 in Fig. 4. The interesting feature is that the shielding factor drops abruptly from 7 to about 4 when the current is increased 2.5 mA after reversal. With a sample-to-coil distance of 1.5 mm this corresponds to a change in applied field of  $\sim 10^{-2}$  Oe. Especially the constant slope after, what might be referred to as a jump or an instability, is unusual. Also as we indicated above, if the current sweep direction is reversed before the slope change, the curve is retraced reversibly. If the current sweep direction is changed after the jump, there is an immediate transition to the lower slope, corresponding to flux trapping or more efficient shielding. As an additional experiment, the current was stopped at a point after the jump. Distinct relaxation was observed. As the current sweep was continued (after, for example, 5s), it was noted that the slope of the SQUID signal had decreased. Thus relaxation makes the shielding more efficient.

At least two features are distinctly different from what would be expected within the framework of Bean's critical state model for homogeneous superconductors:<sup>4</sup> the jumping between varying, but constant levels of shielding, and the relatively large reduction in shielding occurring at the jump. The latter feature is hard to explain, unless the flux penetrates the sample deeply at this point.

In the following we present a qualitative interpretation

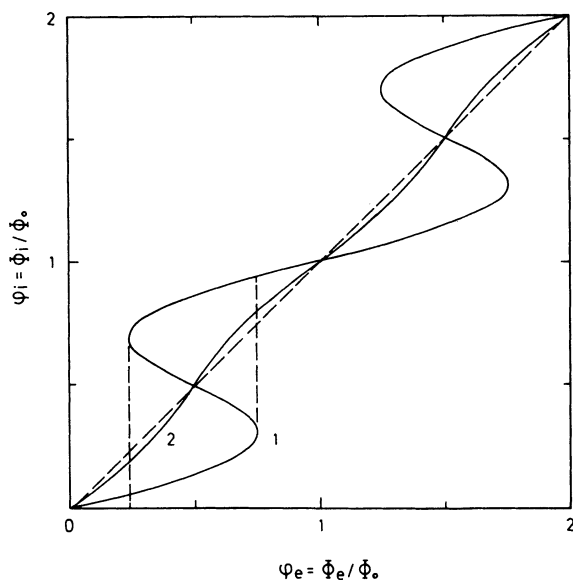


FIG. 5. Total flux ( $\phi_i$ ) versus applied flux ( $\phi_e$ ) for superconducting loop with a Josephson junction.

of the behavior, based on the inhomogeneous nature of the sample. The underlying idea is that the critical current density must be a strongly varying function of both position and field:  $J_C = J_C(\mathbf{r}, \mathbf{B})$ . The position dependence arises from a distribution of weak links between epitaxial islands, and the field dependence is the well-known sharply decreasing critical current of weak links with low, increasing magnetic fields. It is intuitively clear that the interrelation between field and current density contained in this description lead to spin-glass-like behavior with pronounced frustration effects.

The initial, reversible shielding level of  $\sim 7$  we understand as arising from (a) reversible shielding currents in the intergranular regions, (b) from possible normal regions, accessible from the edge, or (c) from the reversible admission of flux through very weak links in the periphery (similar to what happens for an RF-SQUID in the nonhysteretic mode, see Fig. 5). At the jump, we suggest that the increasing field gradient near one or more weak links lifts the current density above the critical value, thus allowing a hysteretic jump. The strong position and field dependence of  $J_C$  will most probably lead to flux penetrating into the center of the sample, as is also observed. In effect, we expect a complicated interplay between changes in current distribution, consequently field, and therefore again current density. The constant shielding level after the jump is attributed to the continuing increasing field, which will ensure that the weak link(s) is (are) open for additional magnetic flux penetrating the sample. On the other hand a decreasing field immediately removes the "magnetic pressure" on the weak link, which then closes. Thus flux is trapped and the higher

level of shielding is reestablished. It seems impossible to account for the observations within continuum models, even with distributions of pinning energies. In a sense, the very small field changes involved reveal the discreteness of the medium.

Moreover, the observed relaxation effects: slow for constant applied field, and fast for decreasing field, where the gradient changes, show that together with a high temperature, the magnetic field plays an important role in the relaxation process.

## V. CONCLUSIONS

We have found indications that defect-rich epitaxial films of high-temperature superconductors display flux dynamics in weak magnetic fields, which are consistent with a description in terms of spin-glass models. Since the critical point is the presence of a high defect level, similar behavior is anticipated in defect low-temperature type-II superconductors. However, because of the lower temperature, other relaxation times are expected.

## ACKNOWLEDGMENTS

We thank A. Kühle for valuable discussions, for providing the defect-rich thin film and the electronmicrograph. V. K. Vlasko-Vlasov and A. A. Polyanskii are acknowledged for characterizing our epitaxial films by the magneto-optical method. The work has been supported by the Danish Materials Research Development Programme under the Ministry of Industrial Affairs.

---

\*Permanent address: Institute of Problems of the Technology of Microelectronics and Highly Pure Materials, Russian Academy of Sciences, Chernogolovka, Moscow district 142432, Russia.

<sup>1</sup>For a review, see, for example, M. Tinkham and C. J. Lobb, *Solid State Physics: Advances in Research and Applications*, edited by H. Ehrenreich (Academic, New York, 1989), Vol. 42, p. 91.

<sup>2</sup>M. Tinkham, *IEEE Trans. Mag.* **27**, 828 (1991).

<sup>3</sup>M. V. Indenbom, Th. Schuster, M. R. Koblishka, A. Forkl, H. Kronmüller, L. A. Dorosinskii, V. K. Vlasko-Vlasov, A. A. Polyanskii, R. L. Prozorov, and V. I. Nikitenko, *Physica C* **209**, 259 (1993).

<sup>4</sup>See, for example, T. van Duzer and C. W. Turner, *Principles of*

*Superconductive Devices and Circuits* (Elsevier, New York, 1981).

<sup>5</sup>See, for example, K. K. Likharev, *Dynamics of Josephson Junctions and Circuits* (Gordon and Breach, Amsterdam, 1986), p. 471.

<sup>6</sup>V. M. Zakosarenko, E. V. Il'ichev, and V. A. Tulin, *IEEE Trans. Mag.* **25**, 946 (1989).

<sup>7</sup>V. M. Zakosarenko, E. V. Il'ichev, and V. A. Tulin, *Pis'ma Zh. Tekh. Fiz.* **15** (1), 7 (1989) [*Sov. Tech. Phys. Lett.* **15**, 3 (1989)].

<sup>8</sup>V. M. Zakosarenko, E. V. Il'ichev, and V. A. Tulin, *Pis'ma Zh. Eksp. Teor. Fiz.* **51**, 275 (1990), [*JETP Lett.* **51**, 315 (1990)].

<sup>9</sup>E. V. Il'ichev, A. V. Andreev, and C. S. Jacobsen, *J. Appl. Phys.* **74**, 3572 (1993).

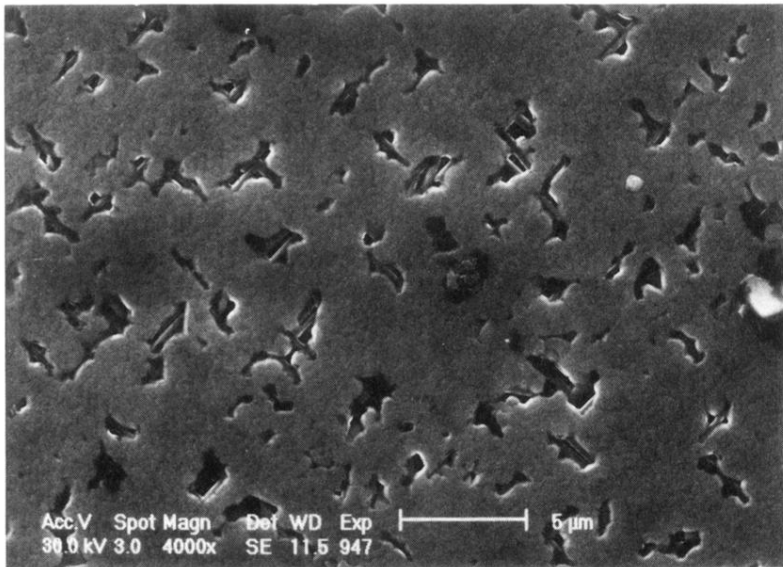


FIG. 2. Scanning electron micrograph of the defect-rich thin film.